Radiation Physics and Chemistry 166 (2020) 108518

Contents lists available at ScienceDirect

Radiation Physics and Chemistry

journal homepage: www.elsevier.com/locate/radphyschem

Microdosimetric calculations by simulating monoenergetic electrons in voxel models of human normal individual cells

Yidi Wang[a,b,c], Zhanpeng Li[a,b,c], Anqi Zhang[a,b,c], Pengcheng Gu[a,b,c], Furong Li[a,b,c], Xiang Li[a,b,c], Wei Tang[a,b,c], Liang Sun[a,b,c,*]

[a] School of Radiation Medicine and Protection, Medical College of Soochow University, Suzhou, 215123, China
[b] State Key Laboratory of Radiation Medicine and Protection, Suzhou, 215123, China
[c] Collaborative Innovation Centre of Radiation Medicine of Jiangsu Higher Education Institutions, Suzhou, 215123, China

A B S T R A C T

This work proposes two kinds of voxel model of human normal individual cells, and the Monte Carlo software GATE is used to describe and analyze the effects of some factors on the microdosimetric quantity–specific energy, such as shape, volume and physical models for interaction. In this paper, “Livermore” and “Penelope”, two of low energy electromagnetic models in the Monte Carlo code Geant4 and adopted in GATE, are used to estimate the specific energies and their distribution of a lung epithelial cell (BEAS-2B), a renal epithelial cell (293T) and their size-like simple ellipsoids (hereinafter referred to as “simple geometry”) respectively. According to the irradiation conditions in radiobiology, four irradiation geometries, the source isotropically irradiated within the cell, the source irradiated axially outside the cell (x-axis positive and z-axis negative) and the cell surface covered with a polypropylene film for external irradiation for monoenergetic electrons beams from 50 keV to 1 MeV are simulated. The results show that the influence of the physical models on the specific energy of the voxel phantom is 27.35% smaller than that of the simple ellipsoid. The BEAS-2B cell shows large differences between phantom and simple geometry in both cytoplasm and nucleus under the condition of external irradiation. For the 293T cell, even if the shape of the cell is relatively regular, there is a deviation between two kinds of geometry under certain conditions, the maximum is 17.78%, while the minimum is 1.19%. These statistical results indicate that shape, volume and position can have a certain impact on the specific energy, and demonstrate that in terms of exploring the mechanism of radiation biological effects, human real cell voxel phantoms may be more practical and valuable than traditional simple models from the aspect of physical modeling. It can be expected that the microdosimetric assessment based on the real cell voxel model and the establishment of relevant databases will play a unique role in predicting the dose of target cell volumes accurately under given conditions in the radiation protection and clinical radiotherapy.

1. Introduction

By observing some phenomena induced by low-dose ionizing radiation, such as target theory (Lea, 1955; Camats et al., 2006), genomic instability (Camats et al., 2006), nontargeted effects (WardJ, 1998; Keith and Belyakov, 2005; Desouky et al., 2015), and bystander effect (Prise, 1998), it is shown that cells, as the basic functional unit of organisms, play an extremely important role in the study of biological effects induced by radiation. Because DNA is the most sensitive target for radiation damage in cells having nanometer dimensions, it is extremely important to understand and simulate the distribution of radiation energy deposition in living cells and subcellular scales.

In 1998, a single-ion irradiation facility developed on the focused horizontal microbeam line of the CENBG 3.5 MV Van de Graaff accelerator (Moretto et al., 2001), which delivered in air single protons and alpha particles of a few MeV onto cultured cells, with a spatial resolution of a few microns (Incerti et al., 2003). Although the spatial resolution of the device is only a few microns, allowing subcellular targeting, it is still impossible to measure the dose of a single cell through experiments directly. This is because cells are in the culture dish, and radiation would be directly deposited in the liquid medium after getting out of the target cells. What's more, the experimental irradiation conditions are very limited, so theoretical calculations and Monte Carlo are generally used to estimate the energy deposition of individual cells. Initially, some simple mathematical geometric volumes were used to replace the shape of cells, such as spheres, cylinders, ellipsoids, etc (Bailly et al., 2002; Jean-Pierre et al., 2002), and water was adopted as the material of cells. Miller (Miller et al., 2000) studied the potential effects of 25–-90 keV electron microbeams on single-cell irradiation, and the results indicate that radiosensitivity was related to the size and shape of cell.

Geant4 (Agostinelli et al., 2003; Allison et al., 2006, 2016) is a Monte Carlo application package based on C++ object-oriented technology that provides tools for importing or defining complex geometry, modeling visualizations, responding to radiation sources in real time, detecting systems and exporting the required output data. GATE is

* Corresponding author. School of Radiation Medicine and Protection, Medical College of Soochow University, Suzhou, 215123, China.
E-mail address: slhmz666@suda.edu.cn (L. Sun).

https://doi.org/10.1016/j.radphyschem.2019.108518
Received 23 July 2019; Received in revised form 14 September 2019; Accepted 5 October 2019
Available online 08 October 2019
0969-806X/

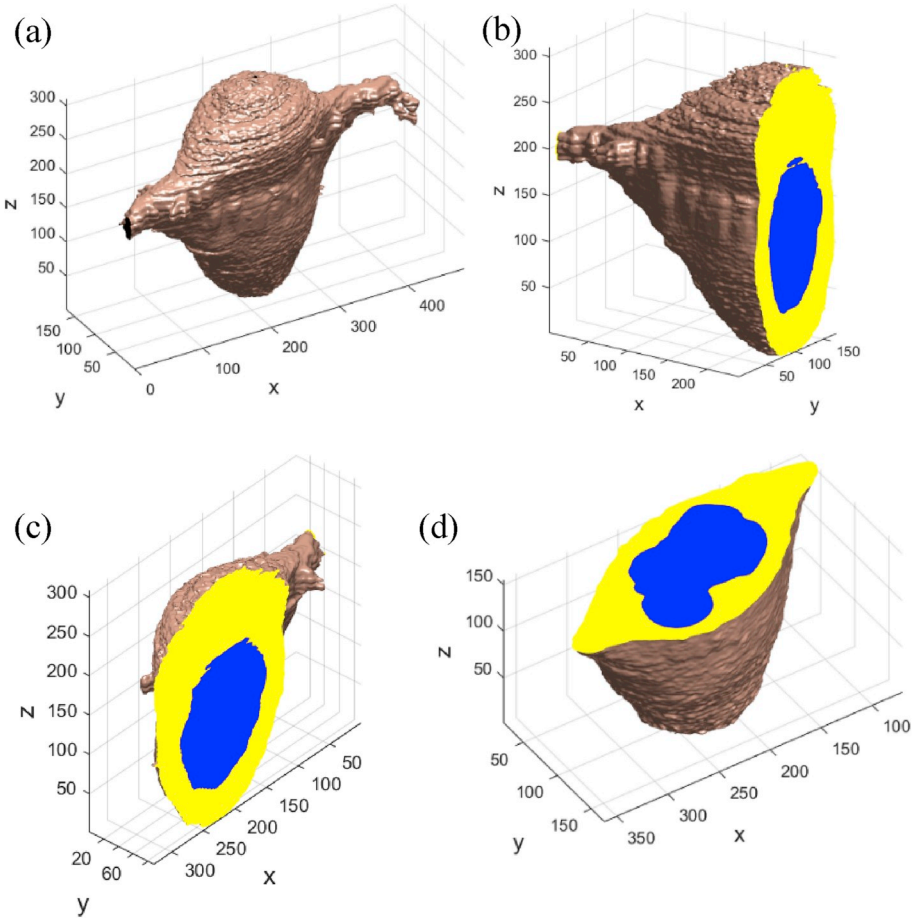

Fig. 1. The stereogram of lung epithelial cells (BEAS-2B) (a), (b) is the profile taken along the vertical plane of the center of the x-axis image; (c) is the profile taken along the vertical plane of the center of the y-axis image; (d) is the profile taken along the vertical plane of the center of the z-axis image. Axis represents the number of voxels in the cell model (unit: pcs).

an advanced opensource software developed by the international OpenGATE collaboration since 2001 and first publicly released in 2004, which dedicated to numerical simulations in medical imaging and radiotherapy. Functions of the platform have been enhanced over the years, and new versions of the software were released on a regular basis, including fully validated upgrades, based on the regular Geant4 public release (Jan et al., 2004; Jan et al., 2011).A large number of studies have used the GATE platform to do voxel phantom calculations on humans or organs (Parach and Rajabi, 2011a,b; Cui et al., 2019). Incerti (Incerti et al., 2003) constructed the CENBG microbeam line device to simulate irradiation at the cell scale using Geant4 toolkit. On this basis, Incerti (Incerti et al., 2009) used confocal microscopy to obtain the three-dimensional voxel of human keratinocytes (HaCaT) and its cell line, and analyzed the chemical composition of the cells by ion beam. Individual cell was irradiated with 3 MeV alpha particles by the CENBG microbeam device based on Geant4. Barberet (Barberet et al., 2012) realized confocal imaging of 76 HaCaT nuclei and determined their chemical composition with IBA. The cell models were imported into Geant4 for two types of irradiation protocols: a 3 MeV alpha particle microbeam used for targeted irradiation and a 239Pu alpha source used for large angle random irradiation. Sihver (Sihver et al., 2014) used the geometry and composition of a real human oral epithelial carcinoma (KB) cell to simulate the energy distribution in the nucleus and cytoplasm based on Geant4. Gao (Gao et al., 2014) investigated the characteristic values about microdosimetry by several situations, including energy, source distributions and source-target combinations.

Low-energy electrons are ubiquitous in the medium or environment under all kinds of irradiation conditions of radiotherapy and radiation protection (Bernal et al., 2015), and secondary electrons generated by high-energy primary ionizing radiation is the primary factor of biological effects, such as DNA molecular strand breaks (Nikjoo et al., 2006). The cellular and subcellular scale of low-energy electrons at the biological tissues are also likely to produce highly localized energy deposition and ionization groups (Camats et al., 2006). Therefore, for exploring the influence of more types of cells on morphology, it is necessary to use electrons as initial particles to record the energy distribution in cell volume.

In this paper, the original cell voxel geometry is obtained by laser confocal microscopy, and geometric input files which GATE could recognize obtained by MATLAB program and VV software. VV is an open-source and cross platform image viewer, designed for fast and simple visualization of spatio-temporal images: 2D, 2D + t, 3D and 3D + t (or 4D) images, runs on Linux, Windows and Mac OS in 32 and 64 bits (VV-the 4D Slice, 2008). GATE version 8.1 “Livermore” and “Penelope” low-energy electromagnetic physics are selected to simulate the large volume of human normal real cells irradiated by monoenergetic electrons, including lung epithelial cells (BEAS-2B) and renal epithelial cells (293T), because real cells are more representative than tumor cells, with initial energy ranging from 50 keV to 1 MeV. In order to evaluate

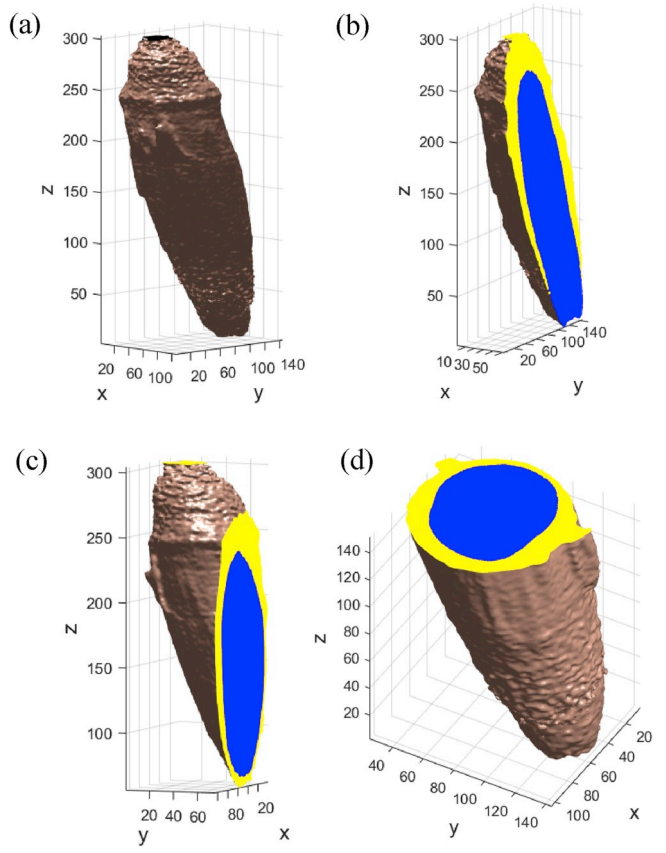

Fig. 2. Same as Fig. 1 for the normal kidney epithelial cells (293T).

Table 1
Parameters of nucleus and cytoplasm in lung epithelial (BEAS-2B) cell and renal epithelial (293T) cell voxel phantoms.

			BEAS-2B	293T
Nucleus	Actual length (um)	x	25.11	14.62
		y	21.33	21.16
		z	25.50	54.20
		Volume (um^3)	5150.62	5242.21
	Axis (um)	x	21.84	14.45
		y	15.82	11.87
		z	23.85	34.00
	Ellipsoid (um)	x	22.00	14.20
		y	18.87	15.84
		z	23.70	44.50
		Volume (um^3)	5151.60	5240.90
	Number of voxels		1160678	885987
Cytoplasm	Actual length (um)	x	82.90	18.23
		y	30.62	25.28
		z	46.50	60.80
		Volume (um^3)	20422.66	4119.76
	Axis (um)	x	34.74	17.03
		y	22.53	16.34
		z	45.00	42.80
	Ellipsoid (um)	x	45.10	16.50
		y	25.00	20.40
		z	43.30	53.12
		Volume (um^3)	25562.00	9362.00
	Number of voxels		4602186	696282
Total	Volume (um^3)		25573.29	9361.97
	Number of voxels		5762864	1582269

differences in microdosimetric quantities between simple models and real voxel phantoms and explore the practicability of GATE in simulating voxel phantom in the field of microdosimetry, we calculate and analyze the energy deposition and microdosimetry quantities of nucleus and cytoplasm. Simple geometric models with the same volume as the real model were established, and the results are compared with those of the real model.

2. Materials and methods

2.1. Voxel phantoms of individual cells

The cell model is originally derived from images of stained cells taken by a laser confocal microscope (Leica TCP-SP). The voxel size is 172 × 172 * 150 nm^3 using the same method as (Sihver et al., 2014). The stained single cell is scanned many times by microscope to get a series of images in tiff format. Then these images are imported into imageJ software to analysis. ImageJ (Collins, 2007) is an open source software which can be extended by plugins and macros using Java. A group of images can be opened in stacks and the actual size of pixels set for all images. The output data of ImageJ include relative coordinates and RGB (red, green, blue) of each voxel, in which case nucleus and cytoplasm can be distinguished because the same material has the same RGB and each voxel is considered as an independent individual.

The cells selected in this paper are human normal lung epithelial cell (BEAS-2B) and renal epithelial cells (293T). Fig. 1 and Fig. 2 show the whole cell image based on voxel three-dimensional matrix and MATLAB self-programming file, whose axis represents the number of voxels in the cell model. Table 1 shows the specific information of the cells and ellipsoids similar with the volume of the cells. Wherein, the "actual length" of x, y, and z are expressed as the length, width, and height of the cuboid that can enclose the nucleus or cytoplasm, and the "actual length" volume is the true length of the cell; the "axis" is the maximum length of nucleus or cytoplasm on a coordinate axis in the three-dimensional coordinate composed of the center point of cell model as the origin; the diameter of the ellipsoid on each coordinate axis is set as a simple geometric model of cell according to the volume and length of the real cell, so that the volume of the ellipsoid is similar to the volume of real cell.

2.2. GATE Monte Carlo simulations

GATE is widely used in the field of nuclear medicine. It is initially devoted to the modeling of plane scintillation scanning, single photon emission computed tomography (SPECT) and positron emission tomography (PET) acquisition, and is widely used in assist PET and SPECT research (Jan et al., 2011). Physic lists were set in GATE according to macro files containing list of command to add physical processes. From GATE version 7.0, it was switched to the "physic list builder" mechanism. Thanks to the addition of electromagnetic physical models, the Geant4 toolkit can more accurately describe the interaction between particles and matter in the low energy domain, especially below the MeV range. The "Livermore" and "Penelope" models enable mixed condensed-history (CH) simulation.

The "Livermore" model is based on EPDL97, EADL public libraries (Perkins et al., 1991; Cullen et al., 1997), which includes the information to determine the cross-section and information needed to describe the final state of each physical interaction. It is applicable to incident electrons and photons, and able to simulate the electron impact ionization, multiple scattering and bremsstrahlung (Incerti et al., 2016), from a few tens of eV up to 100 GeV, with a recommended low

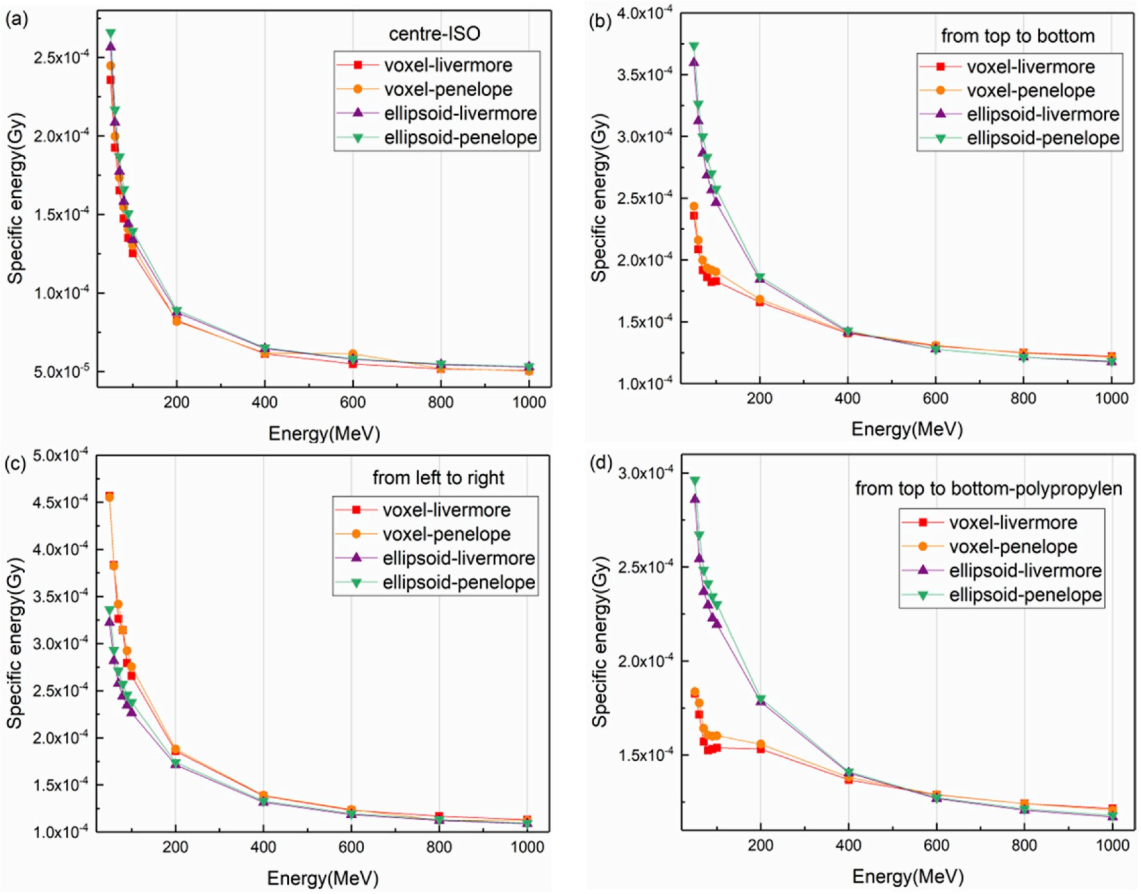

Fig. 3. Specific energy as a function of incident electron kinetic energy, in the nucleus of BEAS-2B and its corresponding simple ellipsoidal geometry for the isotropic irradiation of the source (a), from the left side of the cell to the right (b), from the top side of the cell to the bottom (c), and the cell surface covered with a polypropylene film for external irradiation(d) using the "Livermore" and "Penelope" model in GATE.

energy validity of 250 eV. The theoretical calculation of the electron impact ionization cross section is presented in the EEDL documentation (Perkins et al., 1991). The "Penelope" model is a re-engineering of the PENELOPE 2008 code (J. Baró et al., 1995). The cross-sectional database calculation method for different interaction processes is derived from the work of Seltzer and Berger. It describes the interaction of electrons, positrons, and photons in matter, from tens of eV to 1 GeV, with a recommended minimum energy limit of 100 eV. The ionization model uses the Generalised Oscillator Strength (GOS) model by Liljequist and considers distant longitudinal collisions, distant transverse collisions and close collisions (Liljequist, 1983).

2.3. Geometry input file and operation conditions

In order to achieve the actual cell geometry files that could be read by GATE, the following works are required: Firstly, the voxel files containing coordinates and pixel values obtained by the imageJ software are converted into several DICOM format images using MATLAB program. The pixel of each image is 172 × 172 nm^2, and BEAS-2B cell generates 310 DICOM images, and its pixel matrix of each image is 482 × 178; 293T cell generates a total of 304 DICOM images, and the pixel matrix of each image is 106 × 147. Secondly, DICOM images are imported into VV software and transformed into header files in mhd format and image files in raw format, which could be recognized by GATE version 8.1. (Incerti et al., 2009) demonstrated that material of cells has little effect on energy deposition, so liquid water is used as the main component of cells. The surrounding environment is vacuum in order to reduce the influence of electron scattering on the results, because different distance between external electrons and target cell could cause different electron scattering in other materials.

The initial energies of 10^5 monoenergetic electrons are 50, 60, 70, 80, 90, 100, 200, 400, 600, 800 keV and 1 MeV respectively, which allows maintaining a statistical fluctuation for specific energy below about 1% without exceedingly long simulation times. Simulations begin from 50 keV because it is the lowest energy that electrons could go through the BEAS-2B cell. A production-cut of 2 nm has been applied to all electron simulations. Random seeds are set to a consistent state in order to avoid the deviation of result because of the randomness. Several irradiation environments are considered: isotropic intracellular irradiation, external irradiation along the positive x-axis (from left to right in Figs. 1 and 2), external irradiation along the negative z-axis (from top to bottom in Figs. 1 and 2) and extracellular irradiation in case of a layer of polypropylene on the cell surface, which is most similar to the practical experiments. The geometric method adopted is "nested" parameterization method. In such a 'nested' parameterization, the full parallelepiped is first sliced along the Y vertical axis, each horizontal slice having the same vertical thickness as a single voxel (Incerti et al., 2009). Using GATE version 8.1 based on Geant4 version

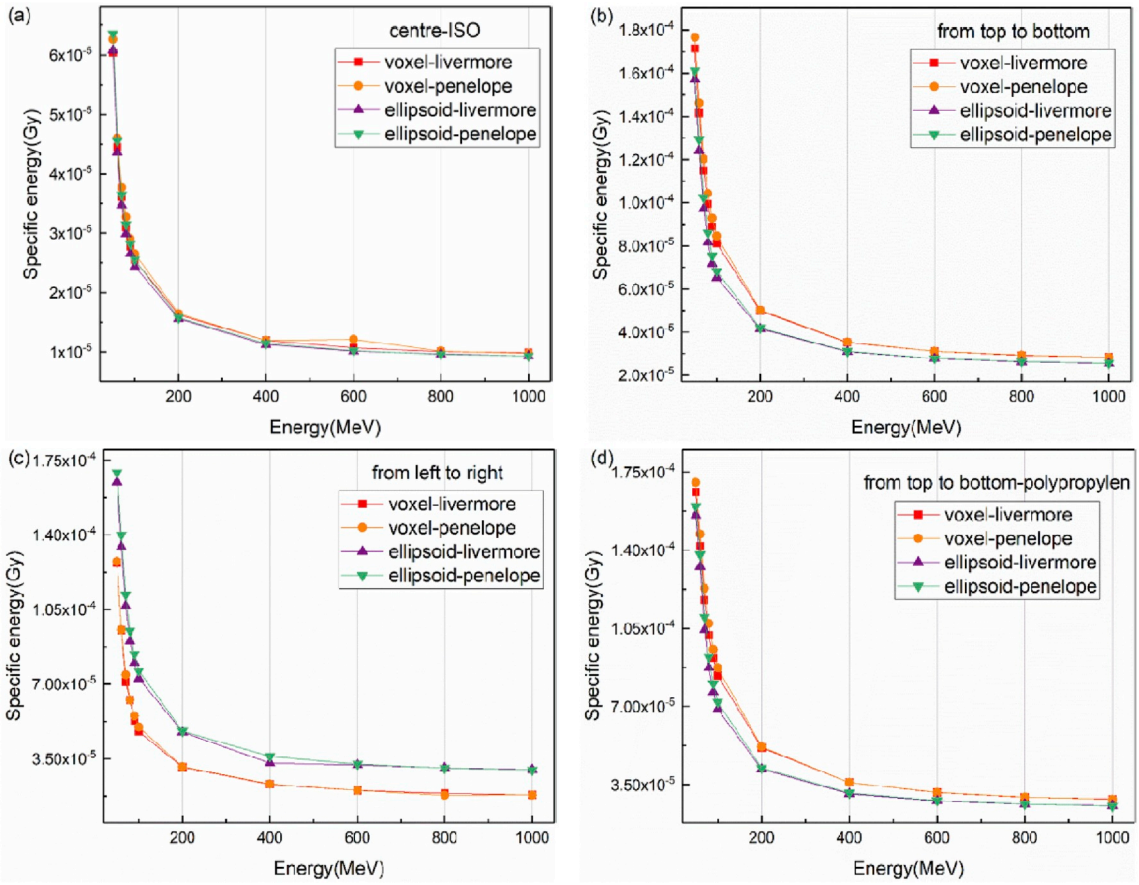

Fig. 4. Same as Fig. 3 for the cytoplasm of BEAS-2B and its corresponding simple ellipsoidal geometry.

10.04.p02, and the computing platform is Intel (R) Xeon (R) E5-2696, 256 GB RAMs high-performance computer.

3. Results and discussion

Specific energy is considered to be an effective physical quantity for evaluating biological effects (Nikjoo et al., 2011). Fig. 3 and Fig. 4 compare the specific energies of nucleus and cytoplasm of BEAS-2B cell. The initial electron energies are 50 keV to 1 MeV and the irradiation conditions are isotropic irradiation in the cell, left to right, top to bottom irradiation and extracellular irradiation in case of polypropylene film on the cell surface. Fig. 5 and Fig. 6 show the specific energy distribution of 293T cell respectively. The irradiation conditions are basically the same as those of BEAS-2B cell. The difference between Figs. 5 (d) and Fig. 6 (d) is that 293T is irradiated from the left to the right after a layer of polypropylene film is covered on the cell surface. It can be found that the results of "Livermore" and "Penelope" are in good agreement, regardless of voxel phantom or simple ellipsoid volume. Through calculation, the relative average deviation of BEAS-2B voxel phantom for these two physical models is 2.47%, and that of corresponding ellipsoid is 2.84%. The relative average deviation of 293T voxel phantom for these two physical models is 1.97%, and the average relative deviation of the corresponding ellipsoid is 2.71%. The number of voxels and the total volume of geometry would have a certain impact on the simulation results of the physical model, and the higher the initial energy, the smaller the relative error.

It can be seen from Figs. 3–6 that the specific energy under various conditions shows that the higher the initial energy, the lower the specific energy, because the high energy electrons have stronger penetrating ability than the low energy electrons, most energy of low-energy electrons can be deposited in the cell volume, while a part of energy of high-energy electrons can pass through the geometric volume directly without depositing energy. It is concluded from part (a) of each figure that the specific energy of cytoplasm and nucleus of voxel phantoms and the ellipsoidal models are in good agreement when the electron source is isotropically emitted at the geometric center, which indicates that energy deposition has a large correlation with the size of the geometry, and the specific energy of nucleus is larger than that of cytoplasm, because of the gradual loss of energy with the transport of particles.

Comparing the curves of various irradiation conditions in Figs. 3 and 4, it is found that the voxel phantom and ellipsoid model have the greatest difference when radiation is irradiated from top to bottom, especially at low energy. This may be due to the irregular shape of the cytoplasm of BEAS-2B cell in the z-axis, which is quite different from the shape of the standard ellipsoid. On the other hand, low-energy electrons have the poor penetration ability in water, the electrons with lower initial energy could not reach the nucleus, their initial particles and secondary electrons will present a more complex track structure in the cytoplasm, while the electrons with higher energy will directly pass

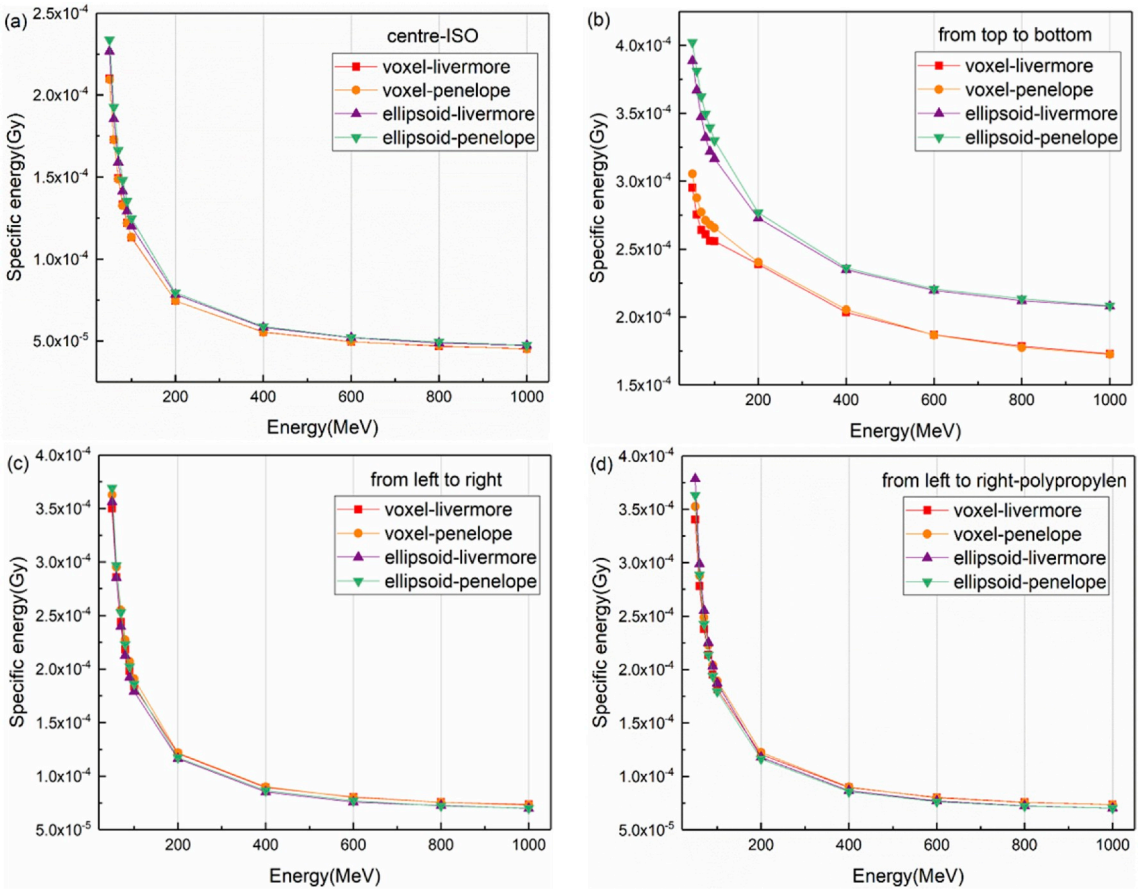

Fig. 5. Specific energy as a function of incident electron kinetic energy, in the nucleus of 293T and its corresponding simple ellipsoidal geometry for the isotropic irradiation of the source (a), from the left side of the cell to the right (b), from the top side of the cell to the bottom (c), and the cell surface covered with a polypropylene film for external irradiation(d) using the "Livermore" and "Penelope" model in GATE.

through the cytoplasm to reach the nucleus.

For 293T cells, although the shape of 293T cell is relatively regular, the difference between cytoplasmic voxel model and corresponding ellipsoid model is relatively large, and the average relative deviation is 17.78%, regardless of the initial energy. This may be because, as shown in Fig. 2, there is a certain deflection in the default position of the 293T voxel model placement, that is, the longitudinal extension line of the cell is not perpendicular to the lateral plane. The energy deposition in the cell body is not only related to the cell, but also has a close relationship with the true shape and placement angle of cells.

For the irradiation conditions of the added polypropylene film, the specific energy of the added polypropylene film is smaller than that non-added polypropylene film, because the particles would lose a certain amount of energy when passing through the film. The maximum specific energy difference is 10.99%, and the minimum difference is 1.19%. In practical experiments, it is necessary to add a layer of polypropylene film to absorb excess water above the cells (Incerti et al., 2003). Therefore, when the cell dose is measured by the actual irradiation device, it is necessary to deduct a certain amount of deviation according to the actual situation. Some average relative deviations of other situations are shown in Table 2, and it only displays the comparison of Livermore since the negligible difference between Livermore and Penelope as shown above.

4. Conclusion

By observing the curve and calculating the relative deviation, it is found that the calculation results of "Livermore" and "Penelope" are in good agreement. Relatively speaking, the selection of the physical model has less influence on the result of the voxel model than that of the simple ellipsoid. The average deviation of cell voxel phantom affected by the physical model is 2.22%, and the geometric model is 2.78%. However, condensed history approach, such as "Livermore" and "Penelope", may not always be appropriate for application to very small volumes because of their longer range of secondary particles. Microdosimetric quantities are very sensitive to the choice of physics model, target size and user-defined simulation parameters. There has been systematic comparison between condensed history and track structure models for users choosing suitable physics model in the simulations (Lazarakis et al., 2018; Kyriakou et al. 2017, 2019). On the other hand, the source irradiated isotropically within the cell has less influence on the two physical models, indicating that the geometric volume is strongly associated with energy deposition, so in this case, it is feasible that simple models are used in the simulation instead of voxel phantoms; while the BEAS-2B cells exhibit great differences in both cytoplasm and nucleus under the condition of extracellular irradiation to the cells, indicating that shape has a high impact on specific energy.

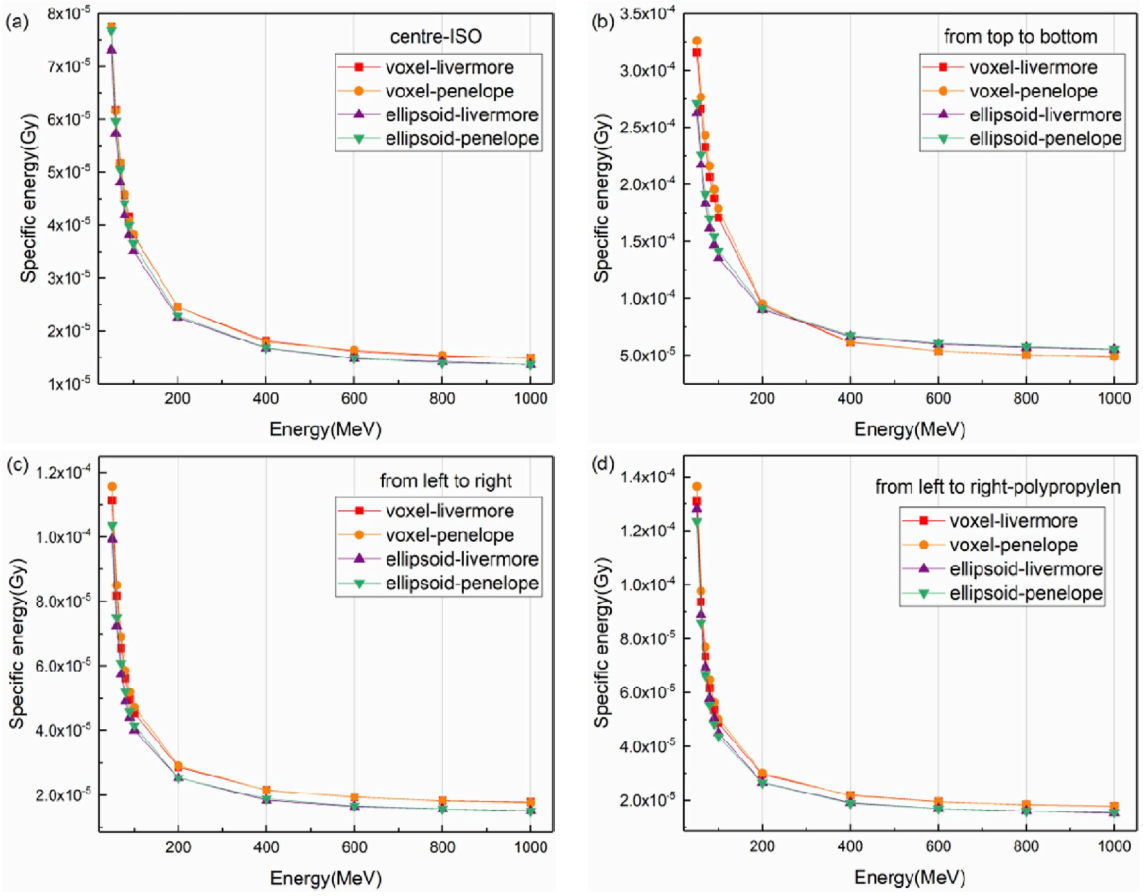

Fig. 6. Same as Fig. 5 for the cytoplasm of 293T and its corresponding simple ellipsoidal geometry.

Table 2
The average relative deviation of specific energy between voxel phantoms and simple ellipsoidal geometries of BEAS-2B and 293T for four kinds of irradiation conditions using Livermore.

		BEAS-2B	293T
centre-ISO	nucleus	6.18%	5.43%
	cytoplasm	4.05%	8.27%
from top to bottom	nucleus	18.72%	18.83%
	cytoplasm	16.43%	17.78%
from left to right	nucleus	17.71%	3.36%
	cytoplasm	33.18%	14.53%
from top to bottom/left to right-polypropylene	nucleus	20.19%	5.05%
	cytoplasm	14.61%	9.61%

When the initial energy is large, the influence of shape on energy is gradually reduced, and the minimum deviation is 3.65%. This is because electrons with larger energy have stronger penetration ability in water. For 293T cells, even if the shape of the cell is relatively regular, there is still 17.78% of the voxel model and simple geometric model when the cells are irradiated from top to bottom. The deviation is due to the angle deviation between the real voxel model and the horizontal plane, which indicates that the energy deposition is also related to the location of cells.

Finally, this work demonstrates the ability to estimate energy deposition in microscopic volumes and to identify complex voxel files using GATE. It indicates that GATE can be used for microdosimetry, laying a solid foundation for simulation of similar community cells in the future. The cell voxel method is also important for building more kinds of cell phantoms.]

Funding

This work was funding by Collaborative Innovation Center of Radiological Medicine of Jiangsu Higher Education Institutions; China funding of the National Natural Science Foundation of China, China (Grant No. 11575124); the Priority Academic Program Development of Jiangsu Higher Education Institutions (PAPD); China and the Nuclear Energy Development Project, China (No. 2016-1295).

Declaration of competing interest

N/A.

References

Agostinelli, S., Allison, J., Amako, K., Apostolakis, J., Araujo, H., Arce, P., Asai, M., Axen, D., Banerjee, S., Barrand, G., 2003. Geant4—a simulation toolkit. Nucl. Instrum. Methods Phys. Res. 506, 250–303.
Allison, J., Amako, K., Apostolakis, J., Araujo, H., Dubois, P.A., Asai, M., Barrand, G., Capra, R., Chauvie, S., Chytracek, R., 2006. Geant4 developments and applications. IEEE Trans. Nucl. Sci. 53, 270–278.
Allison, J., Amako, K., Apostolakis, J., Arce, P., Asai, M., Aso, T., Bagli, E., Bagulya, A.,

Banerjee, S., Barrand, G., 2016. Recent developments in Geant 4. Nucl. Instrum. Methods Phys. Res. 835, 186–225.
Bailly, I., Champion, C., Massiot, P., Savarin, P., Poncy, J.L., Crespin, S., Alloy, G., Jacob, V., Petibon, E., 2002. Development of an experimental system for biological studies: scintillation and solid-track detectors as dose monitors. Nucl. Instrum. Methods Phys. Res. 187, 137–148.
Barberet, P., Vianna, F., Karamitros, M., Moretto, P., Seznec, S.I.H., 2012. Monte-Carlo dosimetry on a realistic cell monolayer geometry exposed to alpha particles. Phys. Med. Biol. 57 (8), 2189–2207.
Baró, J., S, J., M, J., 1995. PENELOPE: an algorithm for Monte Carlo simulation of the penetration and energy loss of electrons and positrons in matter. Nucl. Instrum. Methods Phys. Res. Sect. B Beam Interact. Mater. Atoms 100 (1), 31–46.
Bernal, M.A., Bordage, M.C., Brown, J.M.C., Davídková, M., Delage, E., El Bitar, Z., Enger, S.A., Francis, Z., Guatelli, S., Ivanchenko, V.N., Karamitros, M., Kyriakou, I., Maigne, L., Meylan, S., Murakami, K., Okada, S., Payno, H., Perrot, Y., Petrovic, I., Pham, Q.T., Ristic-Fira, A., Sasaki, T., Štěpán, V., Tran, H.N., Villagrasa, C., Incerti, S., 2015. Track structure modeling in liquid water: a review of the Geant4-DNA very low energy extension of the Geant4 Monte Carlo simulation toolkit. Phys. Med. 31, 861–874.
Camats, N., Ruiz-Herrera, A., Parrilla, J.J., Acien, M., Payá, P., Giulotto, E., Egozcue, J., García, F., Garcia, M., 2006. Genomic instability in rat: Breakpoints induced by ionising radiation and interstitial telomeric-like sequences. Mutat. Res. Fundam. Mol. Mech. Mutagen. 595, 156–166.
Collins, T.J., 2007. ImageJ for microscopy. Biotechniques 43, 25–30.
Cui, T., Li, Z., Zhang, S., Wang, Y., Chen, D., Sun, L., 2019. A comparison between GATE and MCNPX for photon dose calculations in radiation protection using a male voxel phantom. Radiat. Phys. Chem. 157, 47–53.
Cullen, D.E., Hubbell, J.H., Kissel, L., 1997. EPDL97: the Evaluated Photo Data Library 97 Version. Office of Scientific & Technical Information Technical Reports.
Desouky, O., Nan, D., Zhou, G., 2015. Targeted and non-targeted effects of ionizing radiation. J. Radiat. Res. Appl. Sci. 8, 247–254.
Gao, H., Yuan, Y., Mu, L., 2014. Irradiation simulation on virtual cell model by low energy α particle. Atomic Energy Sci. Technol. 48, 1666–1674.
Incerti, S., P Barberet, R Villeneuve, Aguer, P., Gontier, E., Michelethabchi, C., Moretto, P., Nguyen, D.T., Pouthier, T., Smith, R.W., 2003. Simulation of cellular irradiation with the CENBG microbeam line using GEANT4. IEEE Trans. Nucl. Sci. 51, 1395–1401.
Incerti, S., Seznec, H., Simon, M., Barberet, P., Habchi, C., Moretto, P., 2009. Monte Carlo dosimetry for targeted irradiation of individual cells using a microbeam facility. Radiat. Prot. Dosim. 133, 2–11.
Incerti, S., Suerfu, B., Xu, J., Ivantchenko, V., Mantero, A., Brown, J.M.C., Bernal, M.A., Francis, Z., Karamitros, M., Tran, H.N., 2016. Simulation of Auger electron emission from nanometer-size gold targets using the Geant4 Monte Carlo simulation toolkit. Nucl. Instrum. Methods Phys. Res. B 372, 91–101.
Jan, S., Santin, G., Strul, D., Staelens, S., Assié, K., Autret, D., Avner, S., Barbier, R., Bardiès, M., Bloomfield, P.M., 2004. GATE: a simulation toolkit for PET and SPECT. Phys. Med. Biol. 49, 4543.
Jan, S., Benoit, D., Becheva, E., Carlier, T., Cassol, F., Descourt, P., Frisson, T., Grevillot, L., Guigues, L., Maigne, L., 2011. Gate V6: a major enhancement of the GATE simulation platform enabling modelling of CT and radiotherapy. Phys. Med. Biol. 56, 881–901.
Jean-Pierre, A., Véronique, B., Andrei, T., Marie-Laure, N., Jack, A., Sylvain, C., Maryse, R., Pierre, V., Claude, D., 2002. Simulation of neutron interactions at the single-cell level. Radiat. Res. 158, 650–656.
Keith, B., Belyakov, O.V., 2005. Classical radiation biology, the bystander effect and paradigms: a reply. Hum. Exp. Toxicol. 24, 537–542.
Kyriakou, I., Emfietzoglou, D., Ivanchenko, V., Bordage, M.C., Guatelli, S., Lazarakis, P., et al., 2017. Microdosimetry of electrons in liquid water using the low-energy models of Geant4. J. Appl. Phys. 122 (2), 24303.
Kyriakou, I., Ivanchenko, V., Sakata, D., Bordage, M.C., Guatelli, S., Incerti, S., et al., 2019. Influence of track structure and condensed history physics models of Geant4 to nanoscale electron transport in liquid water. Phys. Med. 58, 149–154.
Lazarakis, P., Incerti, S., Ivanchenko, V., Kyriakou, I., Emfietzoglou, D., Corde, S., et al., 2018. Investigation of track structure and condensed history physics models for applications in radiation dosimetry on a micro and nano scale in Geant4. Biomed. Phys. Eng. Express 4 (2), 24001.
Lea, D.E., 1955. Actions of radiations on living cells.
Liljequist, D., 1983. A simple calculation of inelastic mean free path and stopping power for 50 eV-50 keV electrons in solids. J. Phys. D Appl. Phys. 16 (8), 1567–1582.
Miller, J.H., Resat, M.S., Metting, N.F., Wei, K., Lynch, D.J., Wilson, W.E., 2000. Monte Carlo simulation of single-cell irradiation by an electron microbeam. Radiat. Environ. Biophys. 39, 173–177.
Moretto, P., Michelet, C., Balana, A., Barberet, P., Przybylowicz, W.J., Slabbert, J.P., Prozesky, V.M., Pineda, C.A., Brut, G., Laurent, G., 2001. Development of a single ion irradiation system at CENBG for applications in radiation biology. Nucl. Instrum. Methods Phys. Res. 181, 104–109.
Nikjoo, H., Uehara, S., Emfietzoglou, D., Cucinotta, F.A., 2006. Track-structure codes in radiation research. Radiat. Meas. 41, 1052–1074.
Nikjoo, H., Uehara, S., Emfietzoglou, D., Pinsky, L., 2011. A database of frequency distributions of energy depositions in small-size targets by electrons and ions. Radiat. Prot. Dosim. 143 (2–4), 145–151.
Parach, A.A., Rajabi, H., 2011a. A comparison between GATE4 results and MCNP4B published data for internal radiation dosimetry. Nuklearmedizin Nuclear Medicine 50, 122–133.
Parach, A.A., Rajabi, H., 2011b. Assessment of MIRD data for internal dosimetry using the GATE Monte Carlo code. Radiat. Environ. Biophys. 50, 441–450.
Perkins, S.T., Cullen, D.E., Seltzer, S.M., 1991. Tables and Graphs of Electron-Interaction Cross Sections from 10 eV to 100 GeV Derived from the LLNL Evaluated Electron Data Library (EEDL), Z = 1 to 100.
Prise, K.M., 1998. Studies of bystander effects in human fibroblasts using a charged particle microbeam. Int. J. Radiat. Biol. Relat. Stud. Phys. Chem. Med. 74, 793–798.
Sihver, L., Ni, J., Sun, L., Kong, D., Ren, Y., Gu, S., 2014. Voxel model of individual cells and its implementation in microdosimetric calculations using GEANT4. Radiat. Environ. Biophys. 53, 571–579.
VV-the 4D Slice https://www.creatis.insa-lyon.fr/rio/vv/ 2008, 11 March 2017.
WardJ, 1998. In: New Paradigms for Low-Dose Radiation Response in Proceedings of the American Statistical Association Conference on Radiation and Health.